DUCTILE-BRITTLE TRANSITIONS IN THE FRACTURE OF PLASTICALLY-DEFORMING, ADHESIVELY-BONDED STRUCTURES: I EXPERIMENTAL STUDIES

C. Sun[a], M. D. Thouless[b, c], A. M. Waas,[a, b] J. A. Schroeder[d] and P. D. Zavattieri[d]

[a]*Department of Aerospace Engineering*
[b]*Department of Mechanical Engineering*
[c]*Department of Materials Science and Engineering,*
University of Michigan, Ann Arbor, MI 48109, USA

[d]*General Motors Research and Development, 30500 Mound Rd., Warren, MI 48090, USA*

ABSTRACT

Rate effects for adhesively-bonded joints in steel sheets failing by mode-I fracture and plastic deformation were examined. Three types of test geometries were used to provide a range of crack velocities between 0.1 mm/s and 5000 mm/s: a DCB geometry under displacement control, a wedge geometry under displacement control, and a wedge geometry loaded under impact conditions. Two fracture modes were observed: quasi-static crack growth and dynamic crack growth. The quasi-static crack growth was associated with a toughened mode of failure; the dynamic crack growth was associated with a more brittle mode of failure. The experiments indicated that the fracture parameters for the quasi-static crack growth were rate independent, and that quasi-static crack growth could occur even at the highest crack velocities. Effects of rate appeared to be limited to the ease with which a transition to dynamic fracture could be triggered. This transition appeared to be stochastic in nature, it did not appear to be associated with the attainment of any critical value for crack velocity or loading rate. While the mode-I quasi-static fracture behavior appeared to be rate independent, an increase in the tendency for dynamic fracture to be triggered as the crack velocity increased did have the effect of decreasing the average energy dissipated during fracture at higher loading rates.

(October 23, 2007)

I. INTRODUCTION

Adhesive bonding has many advantages over traditional joining techniques for automotive applications. Adhesive bonding is versatile, allowing a range of different materials to be joined. Since the area of contact between two adhesively-bonded adherends is generally larger than the area of contact associated with spot welds or mechanical fasteners, the resultant bond is stiffer, which results in lighter structures [Wagner *et al.*, 1993]. The increased contact area tends to reduce stress concentrations and increase fatigue resistance [Kinloch, 1987]. The high electrical resistivity of most adhesives results in electrical isolation of the adherends in an adhesively bonded structure, with a consequent increase in corrosion resistance. Finally, adhesive bonds allow for an excellent level of surface finish, which is very desirable for a consumer-oriented product such as a car.

The current use of adhesives in the automotive industry is limited because of the lack of a design methodology for adhesively-bonded sheet metal. Historically, fracture mechanics using a single failure parameter of toughness has gained acceptance as the appropriate way of assessing adhesive joints. Unfortunately, the traditional tools of fracture mechanics are inappropriate when large-scale plasticity is exhibited during failure, as is the expected behavior when sheet metal is bonded by adhesives with practical levels of toughness. Under these conditions, cohesive-zone models which use both strength and toughness to characterize an adhesive layer have been found to be very useful for predicting failure of adhesive joints. Mode-I, mode-II and mixed-mode failure of adhesive joints under quasi-static conditions have been successfully modeled by this approach [Yang *et al.*, 1999; Yang & Thouless, 2002; Li *et al.*, 2006]. While there is

strong evidence that cohesive-zone models provide a powerful approach for designing adhesive joints subject to quasi-static loading, understanding the response of adhesive joints to relatively high rates of loading is required before adhesives can be reliably used in automotive applications. Of general concern is the possibility of rate dependence of the adhesive properties. Of particular concern is the possibility of catastrophic loss of toughness at rates that might be appropriate to vehicle crashes. In crashes, it is important that the adhesive maintains significant values of toughness and strength to allow extensive energy dissipation through plastic deformation of the sheet metal.

What we define as quasi-static crack growth occurs when there is a balance between the applied energy-release rate and the energy dissipated by the growth of the crack and associated plastic deformation. Quasi-static crack growth can occur even when the fracture properties are rate dependent. The only requirement is equilibrium between the driving force for crack propagation and the energy dissipated. In other words, we are defining quasi-static crack growth as requiring the input of work by the applied loads. If the energy available for crack growth exceeds the energy associated with the creation of new crack surfaces and plastic deformation of the adherends, the crack will become unstable, and propagate dynamically, with excess energy being shed to dynamic effects such as stress waves. Dynamic crack growth can occur with no additional work being done on the system by the external loads. The interactions between the loading rate, the geometry, and the toughness-velocity relationship can be fairly complex, and can produce a rich set of crack-growth behaviors [Webb and Aifantes, 1995]. For example, crack growth tends to be destabilized when the toughness decreases with an increase in crack velocity. In the absence of rate-dependent values of toughness, crack growth tends to be

unstable under load-control since the energy-release rate often increased with both applied load and crack length. Many practical applications are loaded under displacement-control which tends to be stabilize quasi-static crack growth. However, if there is sufficient elastic energy stored in a body to propagate a crack in the absence of additional work being done by the applied loads, then even displacement-controlled geometries can exhibit unstable behavior [Li *et al.*, 2005].

"Stick-slip" fracture, in which cracks propagate intermittently, when loaded in a steady fashion, have often been observed experimentally [Kinloch and Williams, 1980; Ravi-Chandar and Balzano,1988; Kim and Kim 1988; Kinloch and Yuen 1989]. Sometimes, this "stick-slip" behavior is ascribed to the instability associated with a toughness that decreases with increasing crack velocity [Maugis, 1985; Williams, 1984; Webb and Aifantis, 1995]. An alternative model for stick-slip behavior is the notion of a "crack-initiation toughness" that may be different from a "crack-arrest toughness". For example, plastic deformation ahead of a stationary crack may cause blunting, with a consequent increase in the energy-release rate required to initiate crack growth. Once fracture is initiated, the available energy-release rate exceeds the energy (per unit area of new crack surface) that would be dissipated in the fracture of the adhesive or deformation of adherend. Under displacement control, crack advance eventually results in the energy-release rate dropping below the value required to keep the crack growing (the "crack-arrest toughness"). The crack is then arrested, and the process repeats in a cyclic fashion. Experimental observations interpreted in these terms [Blackman *et al.*, 1995, 1996; Simon *et al.* 2005] seem to indicate that the crack-arrest is relatively insensitive to loading rate, but disappears at low loading rates.

Of particular concern in the present paper are experimental observations of transitions between quasi-static and dynamic fracture in a system that exhibits plastic deformation of the adherends. Developing an understanding of unstable crack growth in the presence of plasticity is crucial for modeling energy management during crashes for adhesive joints in automotive structures. Since plasticity is required to be present for energy absorption, the usual LEFM approaches are not appropriate, and a cohesive-zone approach will be adopted to analyze this phenomenon, as described in the companion paper [Sun *et al.*, 2007]. In the present paper, the experimental observations for the transitions between quasi-static and dynamic fracture in a plastically deforming steel/adhesive/steel structure will be presented. These observations are used in the companion paper to develop a cohesive-zone analysis of the problem, and to determine the appropriate fracture parameters for the adhesive layer. The ultimate goal of this work is to understand the physics of the transition, and to develop numerical models that allow stick-slip behavior to be predicted based on knowledge of the material properties, geometry and loading rates. However, in these initial papers, only the experimental observations and parameter determination are addressed.

II. EXPERIMENTAL RESULTS

1. Tensile tests for the adherend and adhesive

The steel/adhesive/steel specimens used in this research were made by bonding dual-phase steel coupons with a layer of a commercial, rubber-toughened, one part epoxy-based adhesive cured at 180 ºC for thirty minutes. The properties of the steel coupons (after being exposed to an equivalent of the adhesive cure schedule) and the bulk adhesive were obtained from tensile tests using specimens illustrated in Fig. 1 The tests

for the steel were conducted on coupons that were 1.42 ± 0.02 mm thick, under displacement control at nominal rates of 0.05 mm/s, 5 mm/s and 200 mm/s, which corresponded to strain rates up to about 2/s. The strains were monitored by both an extensometer and a strain gauge placed at the center of the specimen. Characteristic nominal stress-strain curves for the steel are shown in Fig. 2, and the material properties are summarized in Table 1. The thickness of the tensile specimens for the bulk adhesive properties was 0.95 ± 0.07 mm. The specimens were prepared by casting thin sheets of the adhesive, and then curing for 30 minutes at 180 ºC. DSC measurements confirmed that the thermal profiles (and the glass-transition temperature) were the same for the bulk adhesive and the adhesive in the bonds. The tensile specimens for the bulk adhesive were tested under displacement control at nominal displacement rates of 0.035 mm/s, 0.50 mm/s, 5.0 mm/s, 50 mm/s and 200 mm/s. The strain was determined from optical images taken with a high-speed camera of thin, equally-spaced lines 20 mm apart that were scribed on the surface before testing, and the load was monitored by a load cell attached to the mechanical testing machine. The resulting nominal stress-strain curves for different ranges of strain rate are presented in Fig. 3, and the tensile properties are summarized in Table 2. These results are shown here, to characterize the constitutive properties of the materials involved in the study. The results are used in the companion paper, as part of the modeling process.

2. Adhesively-bonded double-cantilever beam (DCB) tests

Bonded double-cantilever beam (DCB) specimens of the steel and adhesive were formed with the geometry shown in Fig. 4a. –The thickness of the steel arms was 1.42 ± 0.02 mm, the width was 25.0 ± 0.5 mm, and the total length was 160 mm. "L"-

shaped steel tabs were bonded to the free ends of the specimen to transmit the applied load through a pin joint. The thickness of the adhesive layer was kept at 0.8 ± 0.2 mm for all tests by incorporating glass beads into the adhesive. This thickness was chosen as being characteristic for the bond thickness that might be used in production for the adhesive. The initial length of the crack was defined by Teflon® tape to be 40 ± 2 mm. One side of the beam was painted white and had a scale attached to it, to help determine the location of the crack tip. A high-resolution CCD camera was used to monitor the position of the crack tip, and to calibrate the cross-head displacement. After the tests, striations on the fracture surface were used to estimate the extent of the discrepancy between the location of the crack tip in the middle of the specimen and at the edge. A portion of the quoted experimental uncertainty in the measurements of the crack length is associated with this discrepancy.

The tests were performed using a servo-hydraulic testing machine under displacement control at nominal cross-head displacement rates between 0.1 mm/s and 200 mm/s. Extensive plastic deformation of the steel arms was always observed (Fig. 4b). The specimens failed either by quasi-static crack growth along the entire interface, or by "stick-slip" behavior with the quasi-static crack growth being interrupted by intermittent periods of dynamic fracture. There was no evidence of well-defined critical loading rates being associated with one type of failure or the other. However, transitions to dynamic fracture did appear to be less likely at lower loading rates. Load-displacement curves for the tests that exhibited only quasi-static crack growth are shown in Fig. 5a. In these tests, the load was essentially constant and independent of loading rate, once crack growth began. For this particular geometry and combination of materials, plastic deformation

ensured that the distance from the crack tip to the loading line remained constant, with the crack growing under an approximately constant moment. Load-displacement curves associated with "stick-slip" behavior are shown in Fig. 5b. The drastic drops in load seen in this plot corresponded to regions of dynamic fracture. The gradual drop in the peak load is associated with the fact that plastic deformation was reduced during dynamic fracture, resulting in an increase in the distance between the crack tip and loading line, so a lower load was required for the quasi-static portions of crack growth.

The data of Fig. 5a indicate that the loading rate had a negligible effect on the toughness for quasi-static crack growth.[1] The differences in the load-displacement plots do not appear to be correlated with displacement rates, and are probably associated with minor differences in the adhesive and specimen geometry (such as initial crack length). This is confirmed in the plot of Fig. 6a which shows how the crack lengths vary as a function of the cross-head displacement for the tests that exhibited quasi-static crack growth. These results indicate that the crack velocity was about $68 \pm 2\%$ of the cross-head displacement rate, so the quasi-static crack velocities ranged up to about 140 mm/s. Since all the data for different rates fall on a single master curve, dimensional arguments can be used to show that there were no rate effects for the fracture under this range of conditions. (Furthermore, the linear dependence of crack length on cross-head displacement indicates that the plastic deformation of this geometry results in a steady-

[1] The fact that the total energy dissipation for the joints is independent of rate implies that the toughness of the bond is also independent of rate.

state configuration with the crack growing under an approximately constant bending moment.[2] This is also indicated by the approximately constant load seen in Fig. 5a).

Figure 6b shows an example of how the crack length varied with cross-head displacement when "stick-slip" occurred. The alternating regions of dynamic crack growth and quasi-static crack growth can be seen. It is clear from this figure that the crack growth is not actually "stick-slip" behavior. The crack grows in a quasi-static mode, and then undergoes an abrupt transition to dynamic crack growth. This is believed to be dynamic growth because of the observed oscillations in the load-displacement curve, and because the crack velocity was too fast to be measured even with the 1 ms resolution of the camera. Because the specimen is loaded under displacement control at rates much lower than those that would be required to keep the crack propagating at dynamic speeds, the dynamic crack is eventually arrested. However, the crack then begins growing again in a quasi-static fashion when the displacement (and, hence, load) has increased sufficiently. The quasi-static crack velocities no longer have the same relationship to cross-head displacement rate, because the geometry of the "stick-slip" specimens is changed by the dynamic portions of crack growth, owing to the changes in geometry caused by the different amounts of plastic deformation associated with the two regimes. Visual observations indicated that dynamic fracture is associated with less plastic deformation than quasi-static fracture. This provided quantitative evidence of a lower toughness in the dynamic regime that is confirmed quantitatively in the companion paper (Sun *et al.*, 2007).

[2] Presumably, for very long specimens there would be a gradual transition from the present DCB-like configuration to a T-peel configuration, when the crack velocity would equal the cross-head displacement rate. In the present tests, the geometry appeared to be some way from this transition.

Optical micrographs of the fracture surfaces supported the notion that the quasi-static crack growth regions in the "stick-slip" specimens were identical to the quasi-static crack growth regions in the other specimens, while dynamic fracture was clearly associated with a different mechanism of fracture. Figure 7a shows alternating bands of dark and light surfaces which correlate very well with the extents of alternating quasi-static and dynamic crack growth observed during the experiments. The lighter surfaces are associated with quasi-static fracture; the darker surfaces indicate a smoother fracture surface and are associated with dynamic fracture. Figure 7b shows higher resolution optical micrographs of both types of fracture surface. Surface topology measurements were done using optical interferometry on both types of fracture surface that had been sputter coated by 50-75 nm of Au/Pd. The average roughness of the quasi-static fracture surface was 21 μm, with a standard deviation of 6 μm. The root-mean roughness of the quasi-static fracture surface was 30 μm, with a standard deviation of 10 μm. In contrast to this, the average roughness of the dynamic fracture surface was 13 μm, with a standard deviation of 3 μm. The root-mean roughness of the dynamic fracture surface was 22 μm, with a standard deviation of 6 μm. While there was a statistically significant difference in the topology of the two types of fracture surface, SEM images did not reveal the micro-mechanical origins of the difference in toughness.

3. Wedge tests under displacement control

Wedge tests conducted at similar displacement rates to the DCB tests were performed to establish that the phenomena observed in the previous section are characteristic of the adhesive/steel system rather than the test geometry. The geometry of the specimens is shown in Fig. 8a. The wedge was made of hardened steel. It had an

angle of 10º, a tip diameter of 1 mm, and a length of 120 mm. The bonded end of each specimen was gripped in a servo-hydraulic testing machine and forced over the wedge at a constant nominal velocity between 1 and 250 mm/s, so that the average crack velocities in these wedge tests were similar to the crack velocities obtained with the DCB specimens. The sides of the specimen were painted white to help determine the location of the crack tip more accurately, and a scale was scribed onto the sides. A high-speed camera was focused on the wedge, and the crack velocities and wedge velocity were monitored by comparing the positions of the wedge tip and crack tip to the scale (Fig. 8b). During the tests, the specimens were deformed into the arc of a circle (Fig. 8c), owing to the bending moment imposed by the wedge [Yang *et al.*, 1999].

Tests were done at nominal wedge velocities of 1, 10, 50, 70, 80, 100 and 250 mm/s. The resultant plots of crack extension as a function of time are shown in Fig. 9. Consistent with the observations for the DCB specimens, crack growth was generally quasi-static up to the fastest crack velocities of 250 mm/s. However, three specimens (with average crack velocities of 80 mm/s, 100 mm/s and 250 mm/s) exhibited transitions to dynamic fracture. Although there was evidence of some damage from the wedge passing over the fracture surface, the general color and appearance was the same as the fracture surfaces resulting from the tests of the previous section, with a clear distinction between the regions of quasi-static crack growth and dynamic crack growth. As shown in Fig. 10a, the distance between the crack tip and the wedge was about 7 ± 2 mm for all observed quasi-static crack velocities. The crack jumped to about 13 ± 2 mm ahead of the wedge, when the transition to dynamic fracture occurred (Fig 10b).

4. Wedge tests loaded by dropped weights

Since the range of crack velocities obtained in the DCB and wedge tests were similar, drop-tower tests were performed to obtain higher crack velocities with the same specimen (Fig. 8) and wedge used in the previous tests. A drop weight with a mass of 40 kg was released from heights of 20, 30, 40, 50,100, 500 and 1000 mm onto a bonded coupon sitting on top of a wedge placed 10 mm from the adhesive. This forced the specimen over the wedge at much higher velocities than could be obtained by the earlier experiments. A high-speed camera was focused on the wedge tip, and a scale scribed on the side of the specimen allowed the positions of the crack tip and the wedge relative to the scale to be monitored as a function of time. With the exception of a single test conducted with a drop height of 30 mm drop, "stick-slip" behavior was always observed. In this single exception, only quasi-static crack growth was observed, even at crack velocities in excess of 600 mm/s, until the mass came to rest and the crack was arrested.

Plots of crack extension *versus* time are shown in Fig. 11, from which the average crack velocities were determined to be in the range of about 500 mm/s to 5000 mm/s, depending on the drop height. As a point of comparison, data from the displacement-controlled wedge tests at 250 mm/s have been superimposed on this figure. Figure 11 shows that quasi-static crack growth could be reliably measured at crack velocities up to about 1000 mm/s, and that this quasi-static crack growth was generally punctuated by transitions to dynamic fracture. For the very highest average crack velocities, the time resolution of the camera (1 ms) was insufficient to obtain estimates for the quasi-static crack velocities. However, even with this limitation, there is evidence in Fig. 11 that some quasi-static crack growth, in addition to dynamic fracture, occurred at these highest

rates. This was confirmed by optical observations of the fracture surfaces, that always showed the same alternating patterns associated with transitions between the two failure modes. However, the proportion of fracture surface that corresponded to quasi-static fracture was less than about 10% at the highest velocities. Measurements of the distance between the crack tip and the wedge tip were very consistent with the data obtained from the wedge tests at lower velocities for both quasi-static and dynamic fracture (Fig. 12). Once again, it appears that any possible rate effects for quasi-static crack growth in this adhesive system are smaller than specimen-to-specimen variation, and can be neglected.

The average residual curvatures after fracture for all the wedge specimens (both from the displacement-controlled tests, and from the drop-tower tests) were calculated using the rectangle property of chords and a magnified image of the specimens. The radii of curvature of all specimens that exhibited only quasi-static crack growth was essentially constant and equal to 95 ± 15 mm, irrespective of average crack velocity. There was no correlation with the crack velocity, that was significant beyond specimen-to-specimen variation. This further supported the notion that quasi-static fracture is essentially independent of rate in this system. For the specimens in which transitions to dynamic fracture were observed, the average radii of curvature did tend to increase with an increase in average crack velocity, up to an upper bound of about 550 mm. This was a direct consequence of the fact that the amount of quasi-static crack growth also decreased with average crack velocity. These issues are illustrated in Figure 13. Figure 13a shows how the average curvature varies with crack velocity, and Fig. 13b shows the corresponding relationship between the extent of quasi-static crack growth and average velocity. As is demonstrated in the companion paper [Sun *et al.*, 2007], quasi-static crack

growth dissipates more energy within the adhesive than dynamic fracture. An increase in the energy dissipated within the adhesive results in a corresponding increase in the plastic deformation and curvature of the adherends [Yang *et al.*, 1999]. Therefore, as the average crack velocity increases, the lower toughness mode of fracture dominates, and the average amount of energy dissipated decreases. This has the superficial effect of a rate-dependent toughness. Although, in the present case this appears to arise from transitions between a low and high-toughness failure mechanisms. While the energy dissipation changes with average crack velocity, it does so because of a transition between two growth modes that appear to have essentially rate-independent cohesive properties, not because of a change in toughness with crack velocity for one particular fracture mechanism.

III. CONCLUSIONS

An adhesively-bonded joint formed from a dual phase steel and a commercial adhesive exhibits behavior during fracture with plastic deformation that looks very much like "stick-slip" behavior reported elsewhere for elastic fracture. However, the observations made in the present study provide several features that do not appear to have been addressed before, although they are not inconsistent with previously reported data, and are significant for modeling adhesive fracture at high rates. It appears that the behavior of the adhesive can be described by two modes: a toughened mode and an untoughened mode. In the toughened mode, fracture occurs in a quasi-static fashion. In the untoughened mode, fracture occurs in a dynamic fashion. The fracture properties associated with quasi-static crack growth appear to be essentially independent of crack velocity over a large range of crack velocities up to at least 1000 mm/s.

The effects of rate enter the properties of this system in the form of an instability in the quasi-static crack growth, manifested by a transition to dynamic fracture. This transition appears to be stochastic in nature and to occur more readily at higher loading rates. While the physics for the transition to dynamic fracture is not known, it is clearly not associated with a well-defined critical crack velocity, since quasi-static growth can occur at velocities much in excess of velocities at which transitions to dynamic fracture are observed. Observations from all three sets of experiments presented in this paper indicate that, in this system, toughened quasi-static crack growth could occur at crack velocities of at least 1000 mm/s, but was subject to transitions to dynamic crack growth for crack velocities as low as 50 mm/s. Below this lower bound, toughened, quasi-static fracture appeared to be reasonably stable against transitions to a lower-toughness mode of fracture.

ACKNOWLEDGEMENTS

C. Sun, M. D. Thouless and A. M. Waas gratefully acknowledge the financial support of General Motors. The authors thanks Dr. L. Hector Jr. for helpful discussions regarding surface morphology of fracture surfaces, Dr. M. Lukitsch for obtaining the surface roughness experiments and results quoted in this paper, and Mr. R. Atkins for help with the sample preparation.

REFERENCES

Blackman B. R. K., J. P. Dear, A. J. Kinloch, H. Macgillivray, Y. Wang, J. G. Williams and P. Yayla (1995). "The Failure of Fibre Composites and Adhesively Bonded Fibre Composites under High Rates of Test. I. Mode I Loading - Experimental Studies," *Journal of Material Science*, **30**, 5885-5900.

Blackman B. R. K. A. J. Kinloch, Y. Wang and J. G. Williams (1996). "The Failure of Fibre Composites and Adhesively Bonded Fibre Composites under High Rates of Test. II. Mode I Loading - Dynamic Effects," *Journal of Material Science*, **31**, 4451-4466.

Kim K. S. and J. Kim (1988). "Elasto-Plastic Analysis of the Peel Test for Thin Film Adhesion," *Journal of Engineering and Materials Technology*, **110**, 266-273.

Kinloch A. J. (1987). *Adhesion and Adhesives: Science and Technology*. Chapman and Hall, London.

Kinloch A. J. and J. G. Williams (1980). "Crack Blunting Mechanisms in Polymers," *Journal of Materials Science*, **15**, 987-996.

Kinloch A. J. and M. L. Yuen (1989). "The Mechanical Behaviour of Polyimide-Copper Laminates part 2: Peel Energy Measurements," *Journal of Adhesion*, **30**, 151-170.

Li S., M. D. Thouless, A. M. Waas, J. A. Schroeder and P. D. Zavattieri (2005). "Use of a Cohesive-Zone Model to Analyze the Fracture of a Fiber-Reinforced Polymer-Matrix Composite," *Composites Science and Technology,* **65**, 537-549.

Li S., M. D. Thouless, A. M. Waas, J. A. Schroeder and P. D. Zavattieri (2006). "Mixed-Mode Cohesive-Zone Models for Fracture of an Adhesively-Bonded Polymer-Matrix Composite," *Engineering Fracture Mechanics*, **73**, 64-78.

Maugis, D. (1985). "Review Subcritical Crack Growth, Surface Energy, Fracture Toughness, Stick-Slip and Embrittlement," *Journal of Materials Science*, **20**, 3041-3073.

Ravi-Chandar K. and M. Balzano (1988). "On the Mechanics and Mechanisms of Crack Growth in Polymeric Materials," *Engineering Fracture Mechanics*. **30**, 713-727.

Simon J. C., E. Johnson and Dillard DA (2005). "Characterizing Dynamic Fracture Behavior of Adhesive Joints under Quasi-static and Impact Loading," *Journal of ASTM International,* **2**, 467-484.

Sun C., M. D. Thouless A. M. Waas, J. A. Schroeder and P. D. Zavattieri (2007). "Mode-I, Stick-Slip Fracture in Plastically-Deforming, Adhesively-Bonded Structures: II Numerical Studies," submitted to *International Journal of Solids and Structures*.

Wagner D. A., C. M. Cunningham and M. A. Debolt (1993). "Weld Bonded Joint Design: Pickup Box Case Study," *Proceedings of the International Body Engineering Conference*, 123-128.

Webb T. W and E. C. Aifantis (1995). "Oscillatory Fracture in Polymeric Materials," *International Journal of Solids and Structures,* **32**, 2725-2743.

Williams J. G. (1988). "Transient Effects during Rapid Crack Propagation," *International Journal of Fracture*, **93**, 51-61.

Yang Q. D, M. D. Thouless and S. M. Ward (1999). "Numerical Simulations of Adhesively Bonded Beams Failing with Extensive Plastic Deformation," *Journal of the Mechanics and Physics of Solid*s, **47**, 1337–1353.

Yang Q. D. and M. D. Thouless (2001). "Mixed-Mode Fracture Analyses of Plastically-Deforming Adhesive Joints," *International Journal of Fracture*, **110**, 175-187.

Table 1: Properties of the steel adherends

Nominal strain rate(/s)	Young's modulus (GPa)	Ultimate tensile strength (MPa)	Yield stress, MPa (0.1% offset)
~ 0.0007	193 ± 8	630 ± 1	410 ± 1
~ 0.07	209 ± 10	651 ± 1	425 ± 3
~ 2	216 ± 7	674 ± 3	446 ± 4

Table 2: Properties of the bulk adhesive

Nominal strain rates (/s)	Young's modulus (GPa)	Ultimate tensile strength (MPa)
0.0006~ 0.01	0.9 ± 0.2	29.9 ± 2.5
0.07~ 0.2	1.6 ± 0.6	39.0 ± 1.9
1~ 5	1.8 ± 0.6	45.4 ± 1.8

List of Figures

Figure 8 **(a)** Geometry of the wedge-test specimens, and wedge used in this study. **(b)** Photograph of the experimental configuration for the wedge tests. **(c)** A micrograph of a wedge specimen after fracture at a nominal wedge velocity of 80 mm/s.

Figure 9 Plot of crack extension against time for different nominal wedge velocities. The uncertainties for measurements of the crack length are ± 1 mm.

Figure 10 Plot of crack length ahead of the wedge tip against crack extension for **(a)** tests that exhibited only quasi-static crack growth, and **(b)** tests that exhibited some regions of dynamic fracture. The uncertainties for measurements of the crack length are ± 1 mm.

Figure 11 Plot of crack extension against time for different drop heights. The uncertainties for measurements of the crack length are ± 1 mm.

Figure 12 Plots of crack length ahead of the wedge tip against crack extension for the quasi-static crack growing at about 600 mm/s in the drop tower tests, and for some examples of "stick-slip" crack growth obtained from the drop tower tests.

Figure 13 **(a)** Plot of average curvature against average crack velocity for the wedge and drop tower tests. **(b)** Plot of fraction of quasi-static crack growth as a function of average crack velocity for the wedge and drop tower tests.

.

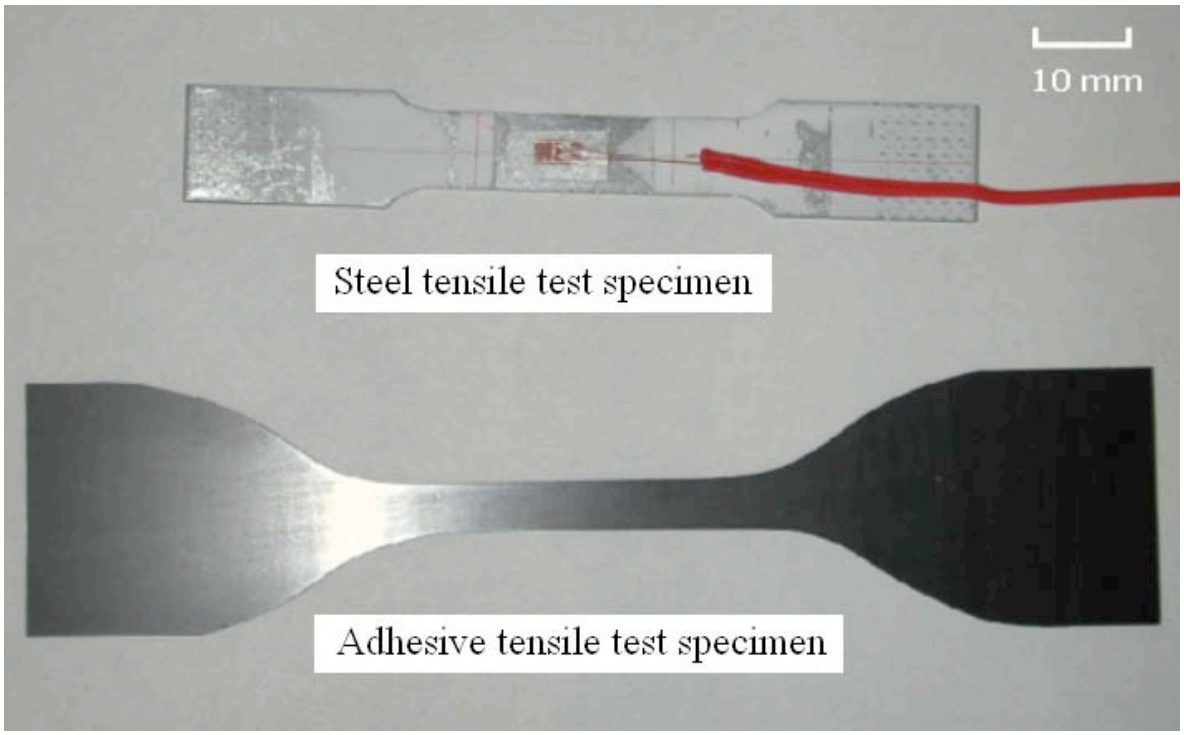
10 mm
Steel tensile test specimen
Adhesive tensile test specimen

Figure 1 .

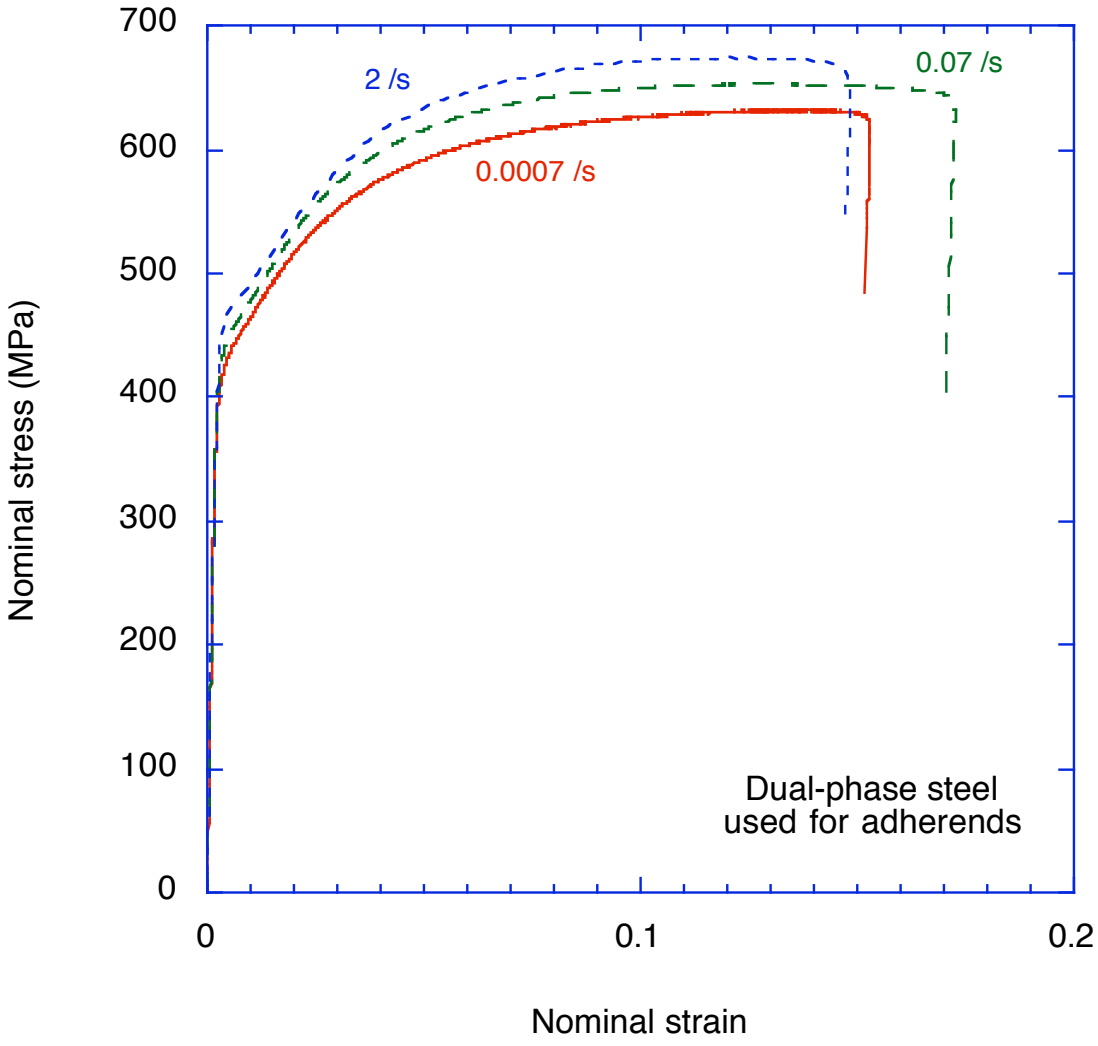
700
600
500
400
300
200
100
0
0
0.1
0.2
Nominal stress (MPa)
Nominal strain
2 /s
0.07 /s
0.0007 /s
Dual-phase steel
used for adherends

Figure 2

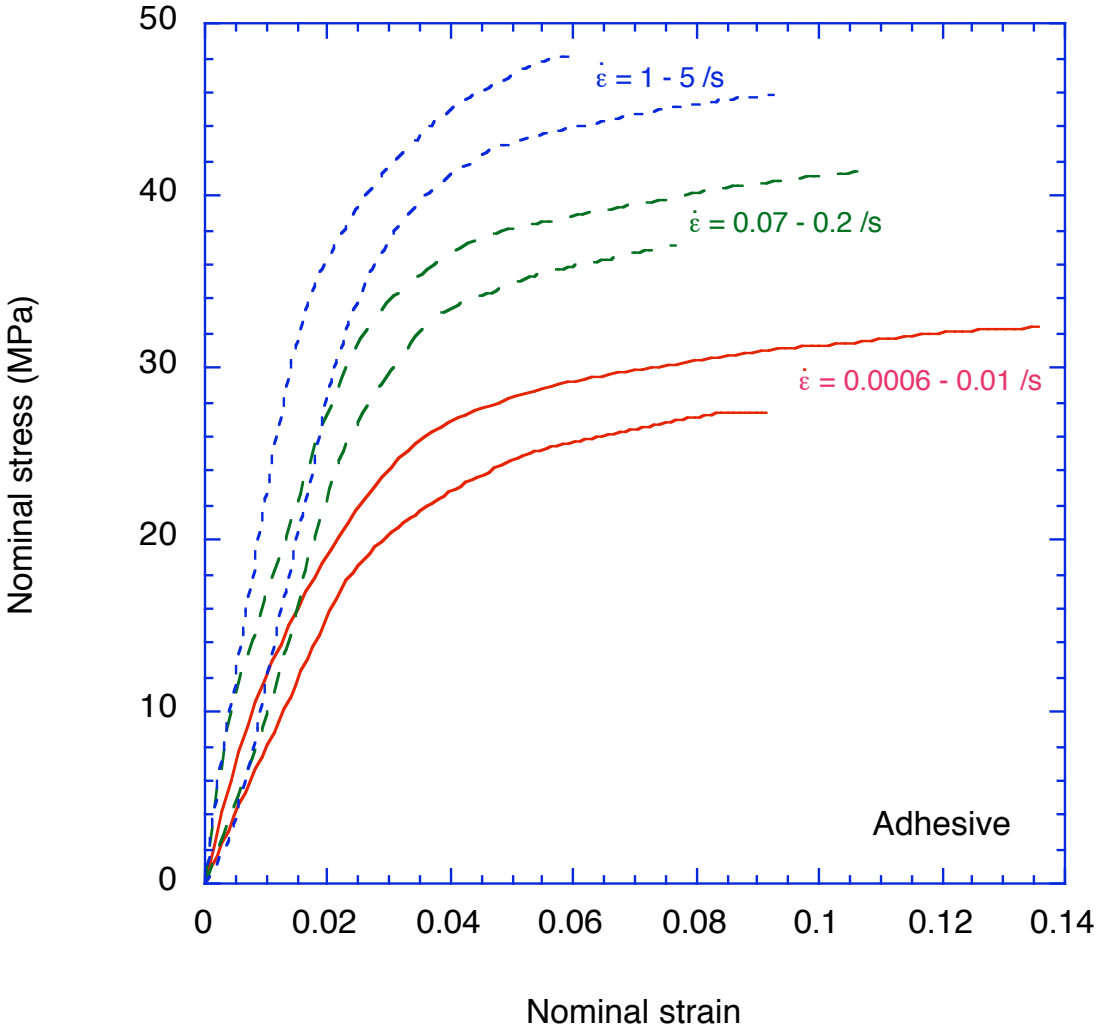
50
40
30
20
10
0
0
0.02
0.04
0.06
0.08
0.1
0.12
0.14
Nominal stress (MPa)
Nominal strain
ε̇ = 1 - 5 /s
ε̇ = 0.07 - 0.2 /s
ε̇ = 0.0006 - 0.01 /s
Adhesive

Figure 3

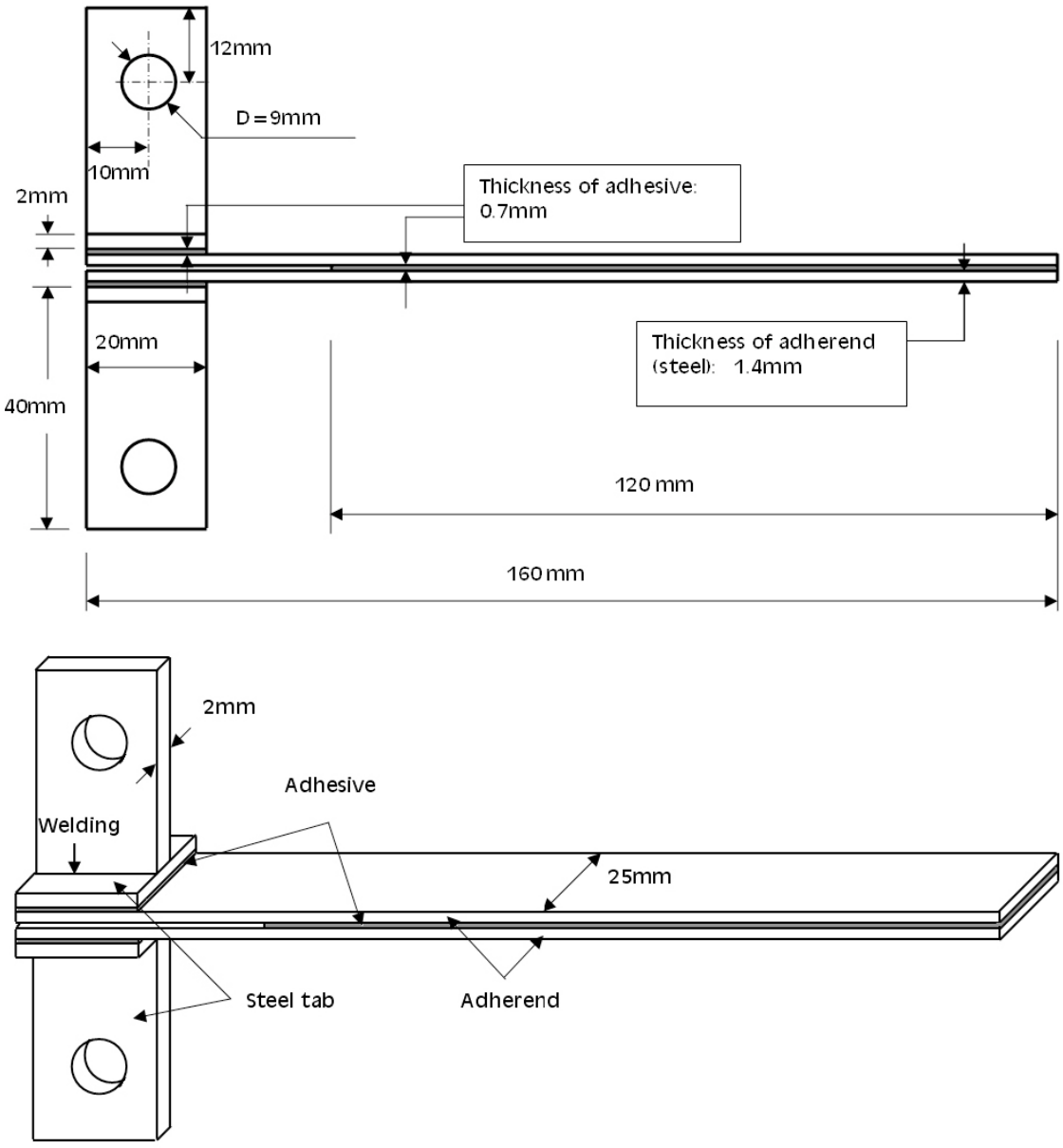
12mm
D=9mm
10mm
2mm
Thickness of adhesive:
0.7mm
20mm
40mm
Thickness of adherend
(steel): 1.4mm
120 mm
160 mm
2mm
Adhesive
Welding
25mm
Steel tab
Adherend

Figure 4a

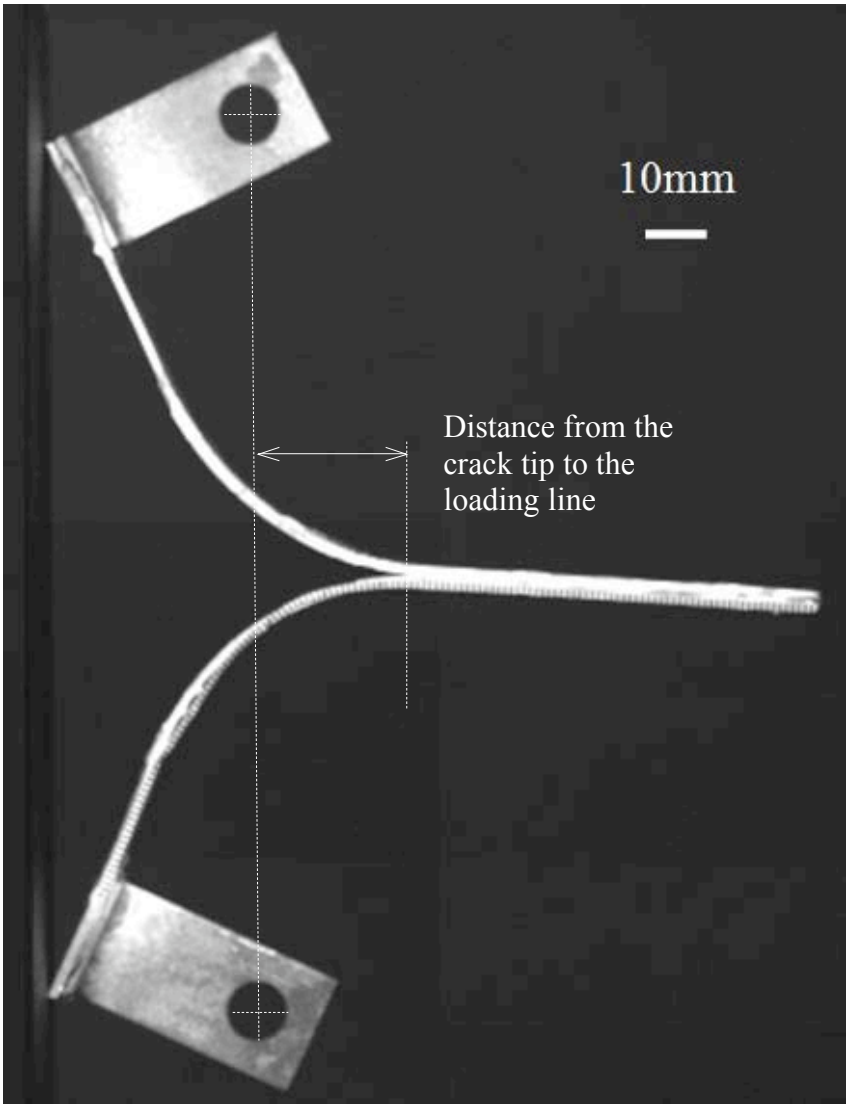

Figure 4b

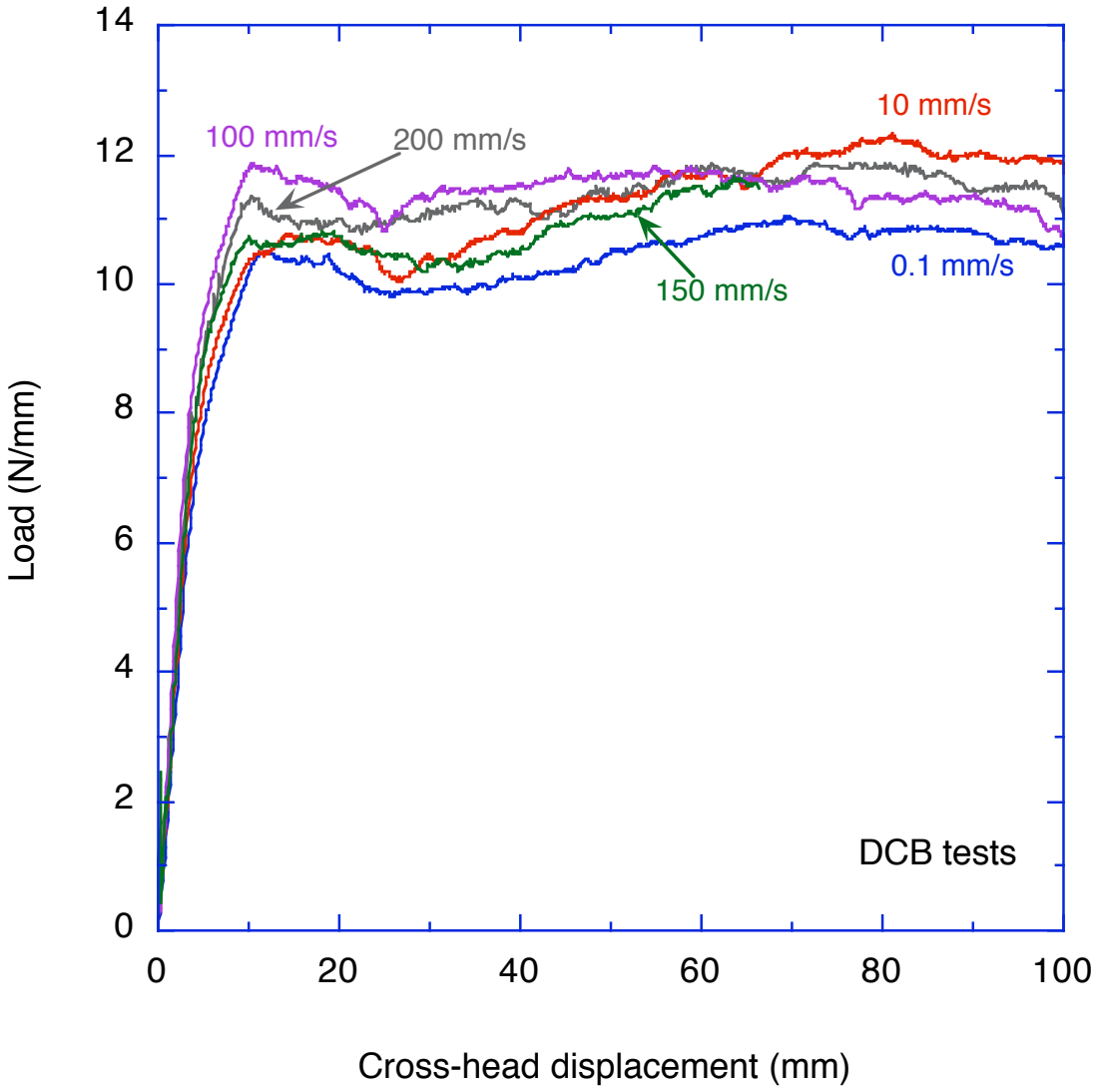
14
12
10
8
6
4
2
0
0
20
40
60
80
100
Load (N/mm)
Cross-head displacement (mm)
100 mm/s
200 mm/s
10 mm/s
0.1 mm/s
150 mm/s
DCB tests

Figure 5a

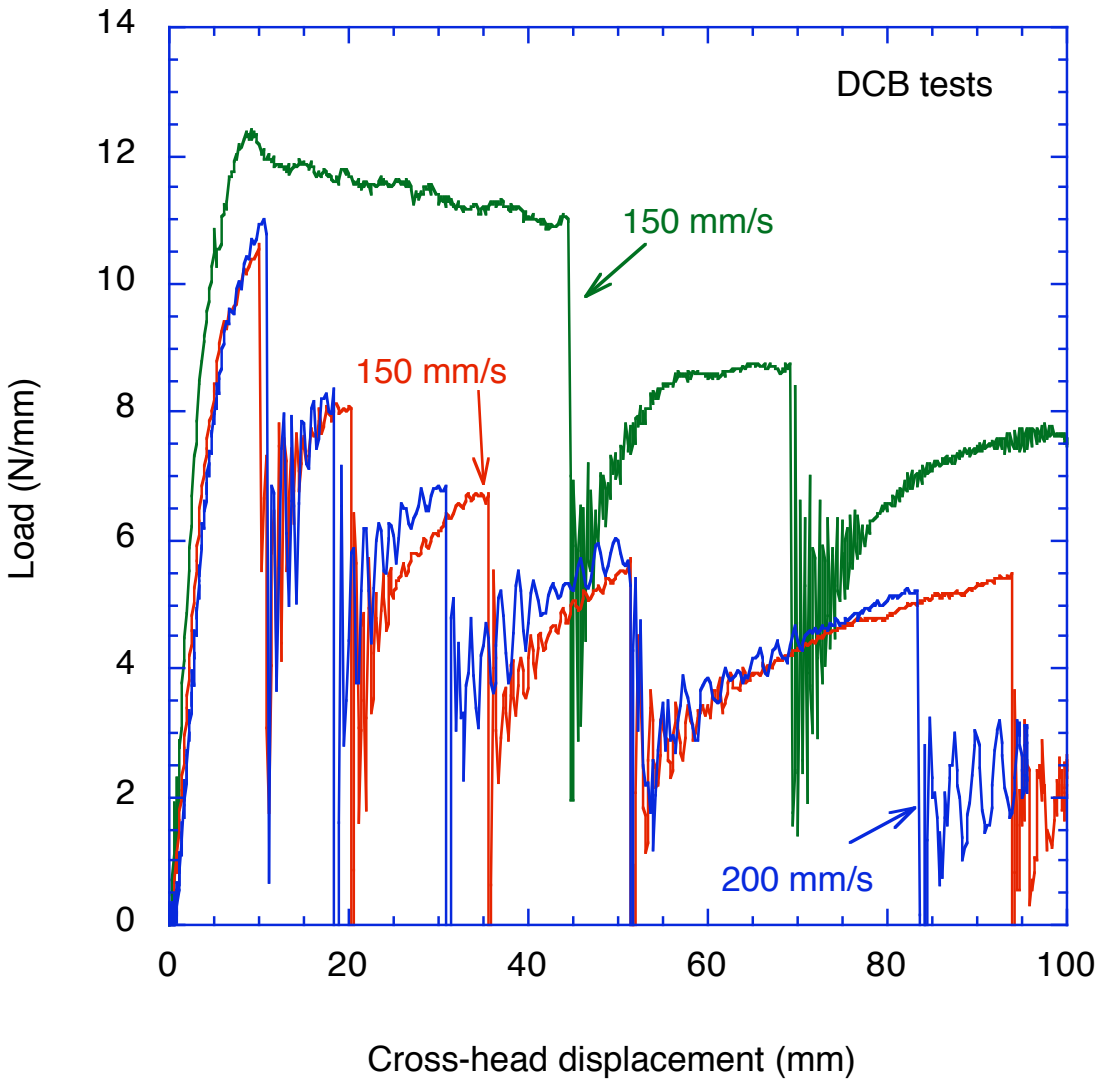
DCB tests
150 mm/s
150 mm/s
200 mm/s
Load (N/mm)
Cross-head displacement (mm)
0
2
4
6
8
10
12
14
0
20
40
60
80
100

Figure 5b

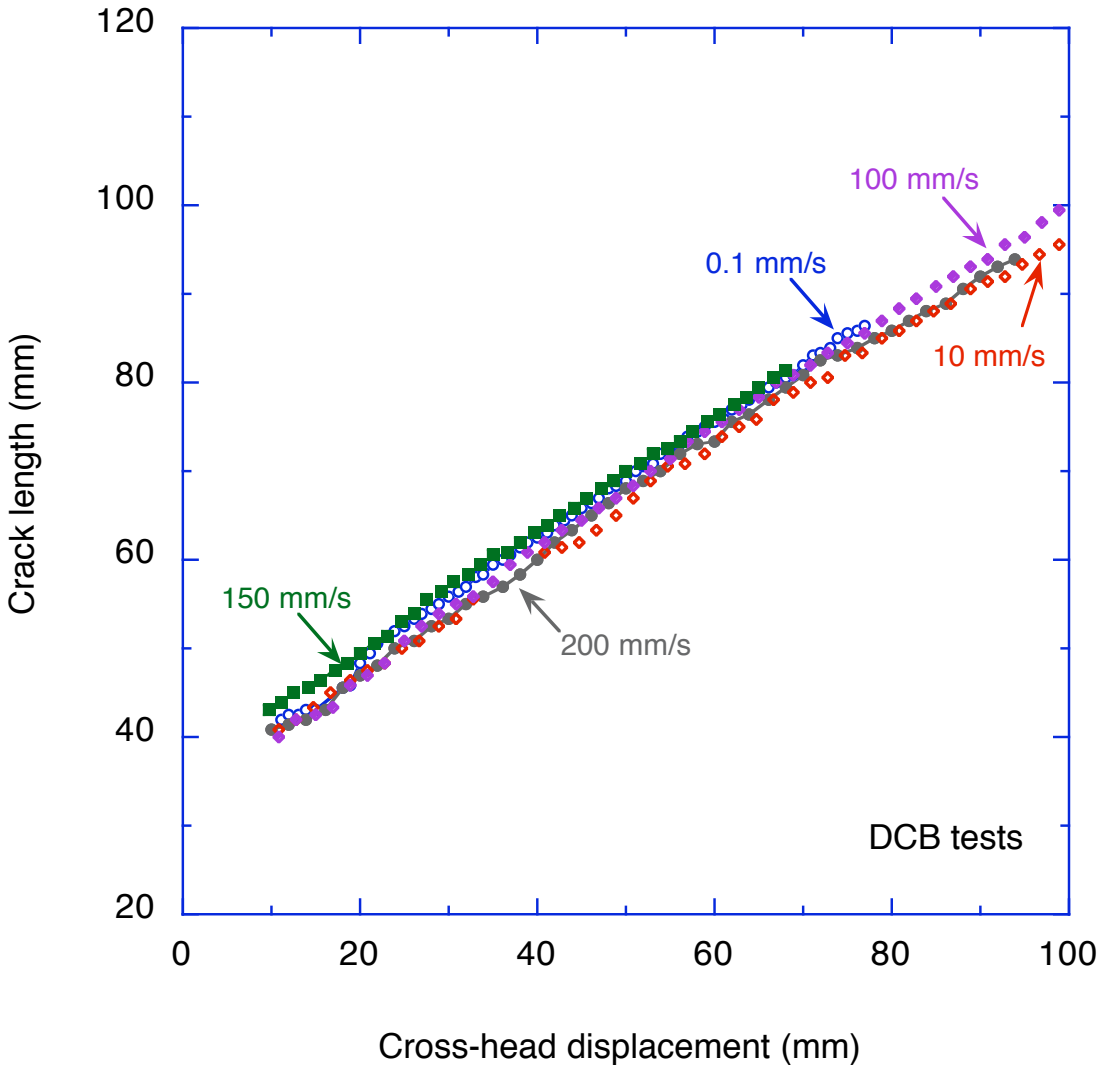
120
100
80
60
40
20
0
20
40
60
80
100
Crack length (mm)
Cross-head displacement (mm)
100 mm/s
0.1 mm/s
10 mm/s
150 mm/s
200 mm/s
DCB tests

Figure 6a

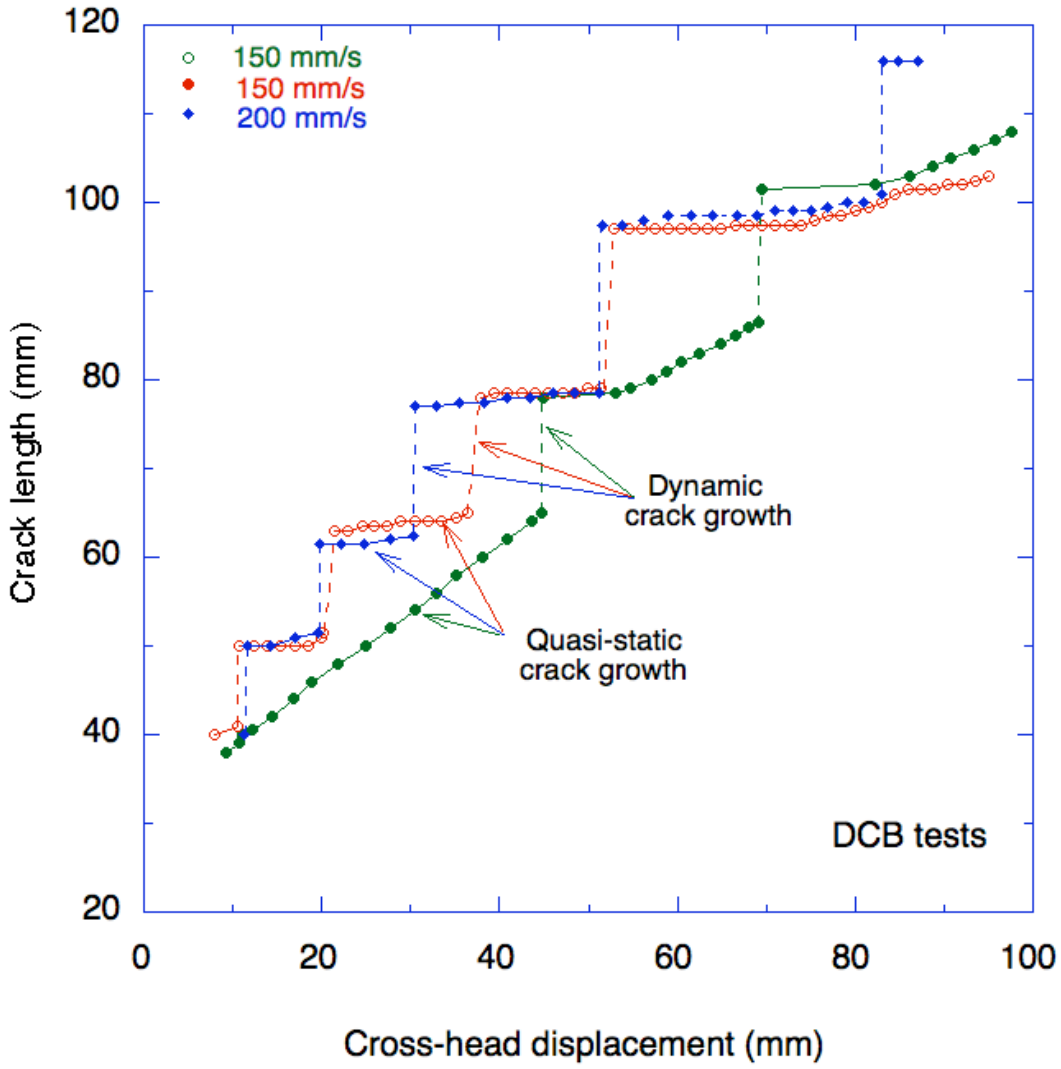
150 mm/s
150 mm/s
200 mm/s
Dynamic
crack growth
Quasi-static
crack growth
DCB tests
Crack length (mm)
Cross-head displacement (mm)
120
100
80
60
40
20
0
20
40
60
80
100

Figure 6b

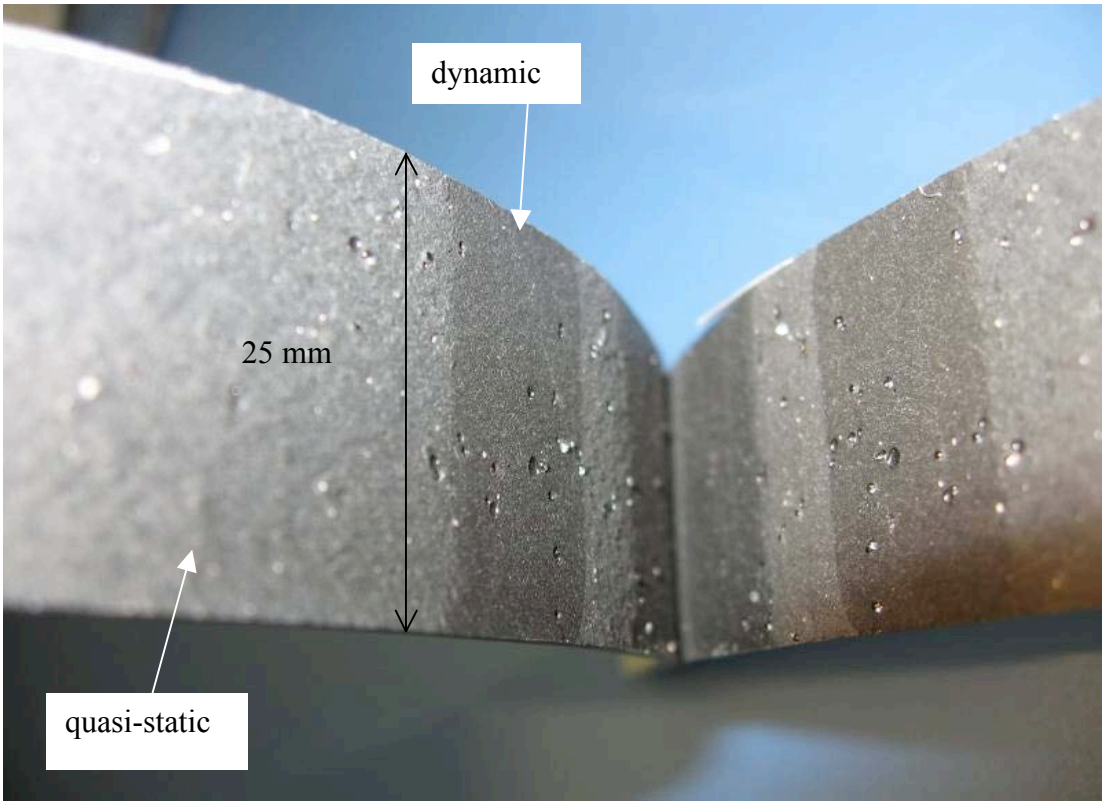

Figure 7a

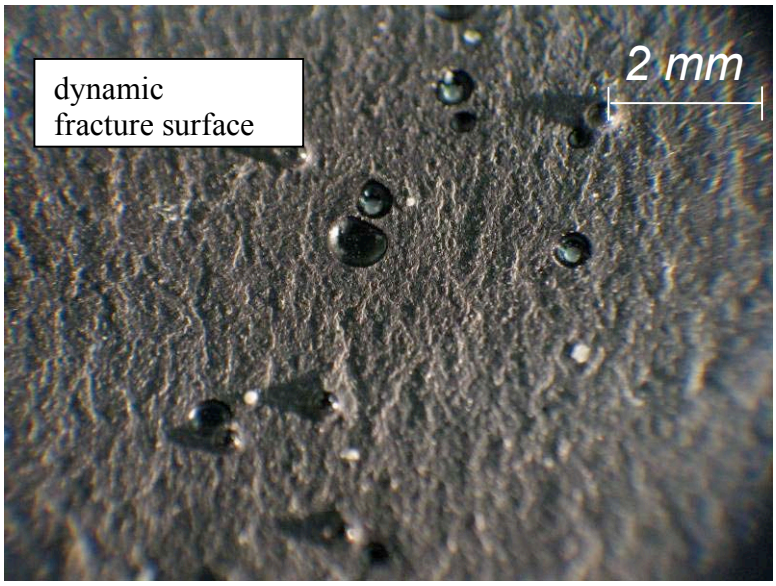
dynamic
fracture surface
2 mm

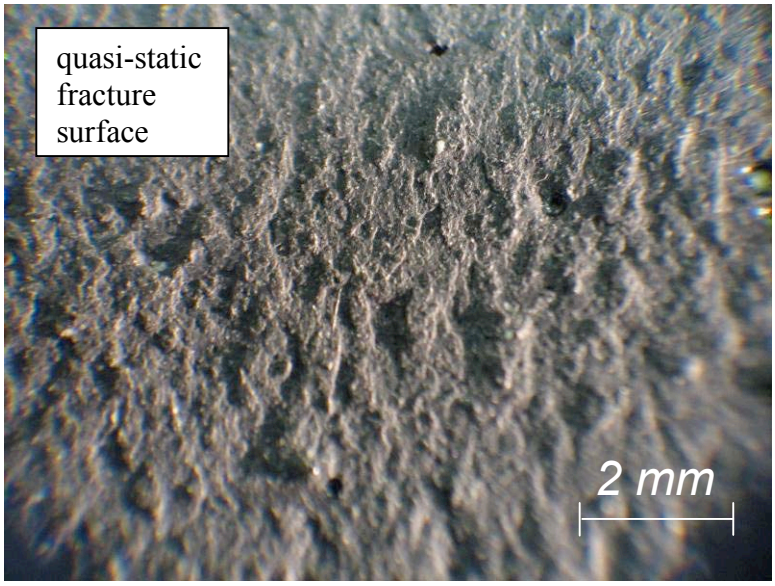
quasi-static
fracture
surface
2 mm

Figure 7b

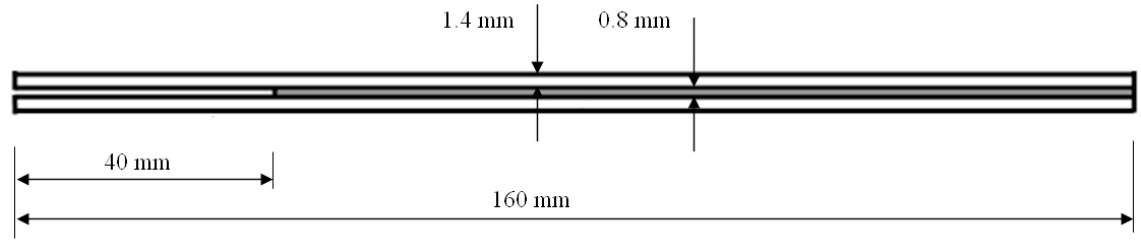
1.4 mm
0.8 mm
40 mm
160 mm

(a)

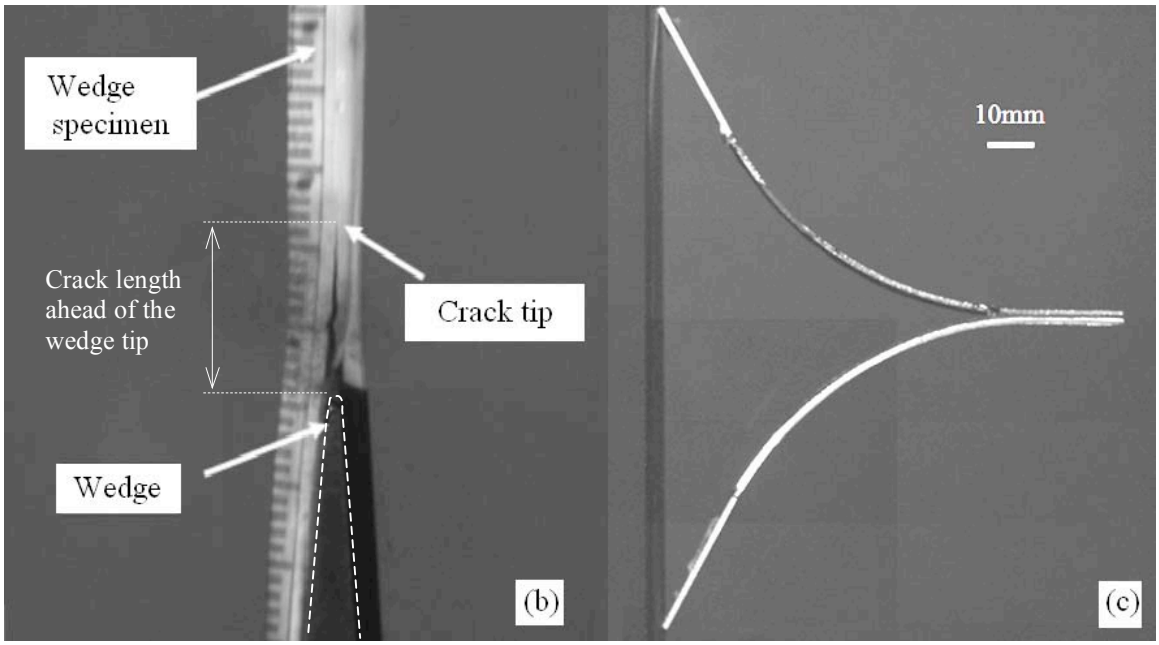
Wedge specimen
Crack length ahead of the wedge tip
Crack tip
Wedge
(b)
10mm
(c)

Figure 8

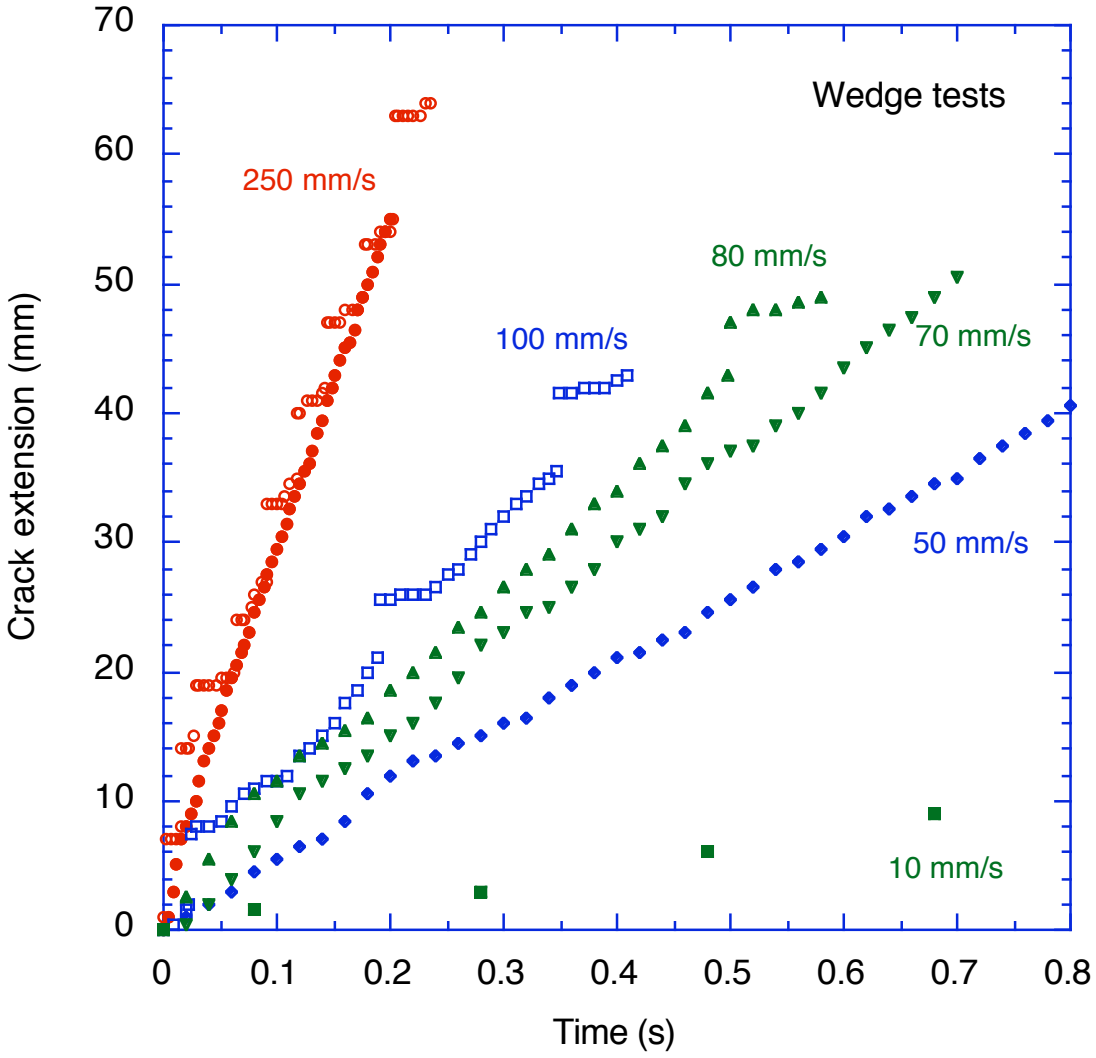
Wedge tests
250 mm/s
100 mm/s
80 mm/s
70 mm/s
50 mm/s
10 mm/s
Crack extension (mm)
Time (s)
0
10
20
30
40
50
60
70
0
0.1
0.2
0.3
0.4
0.5
0.6
0.7
0.8

Figure 9

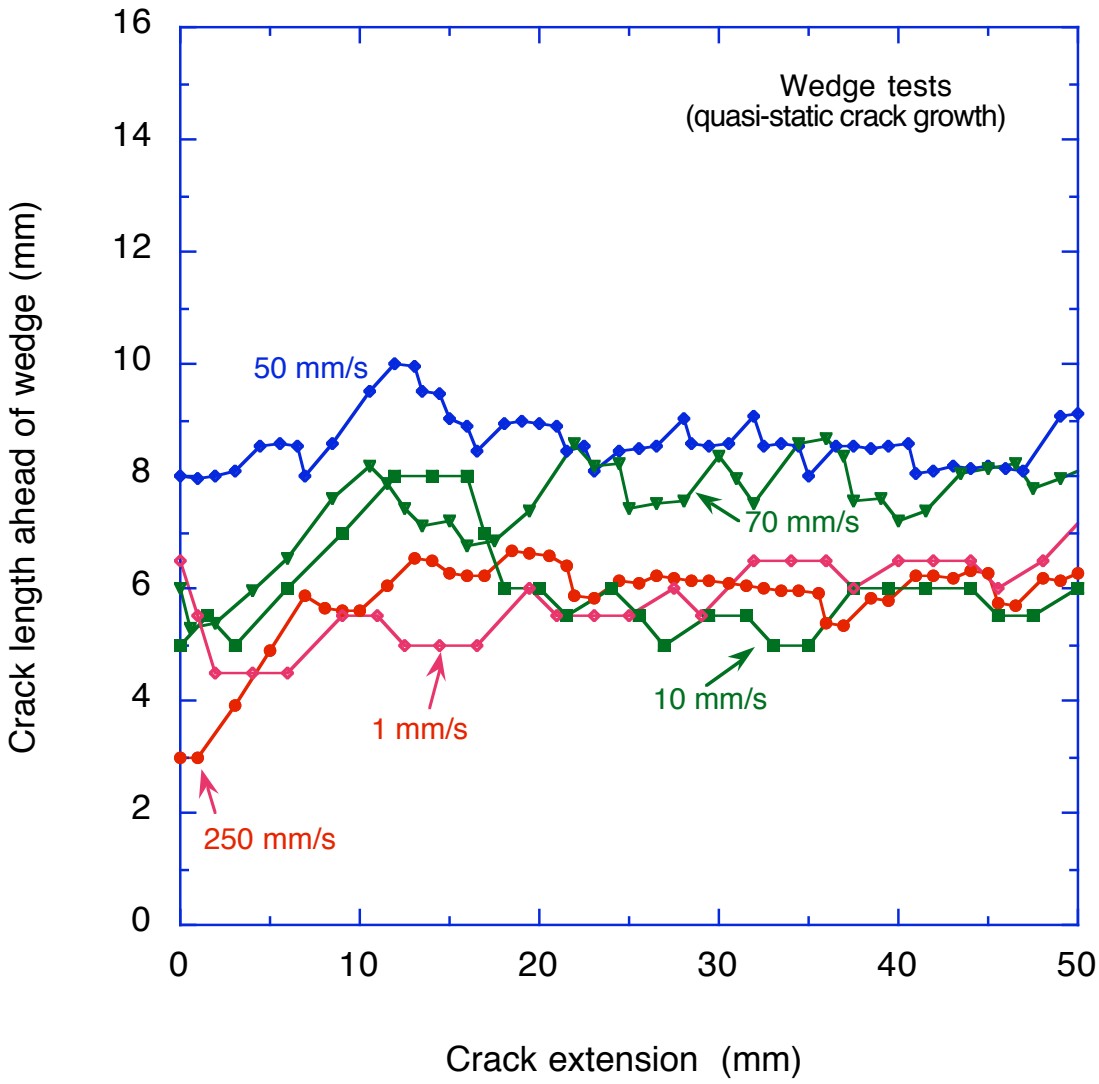
Wedge tests
(quasi-static crack growth)
50 mm/s
70 mm/s
10 mm/s
1 mm/s
250 mm/s
Crack length ahead of wedge (mm)
Crack extension (mm)
0
2
4
6
8
10
12
14
16
0
10
20
30
40
50

Figure 10a

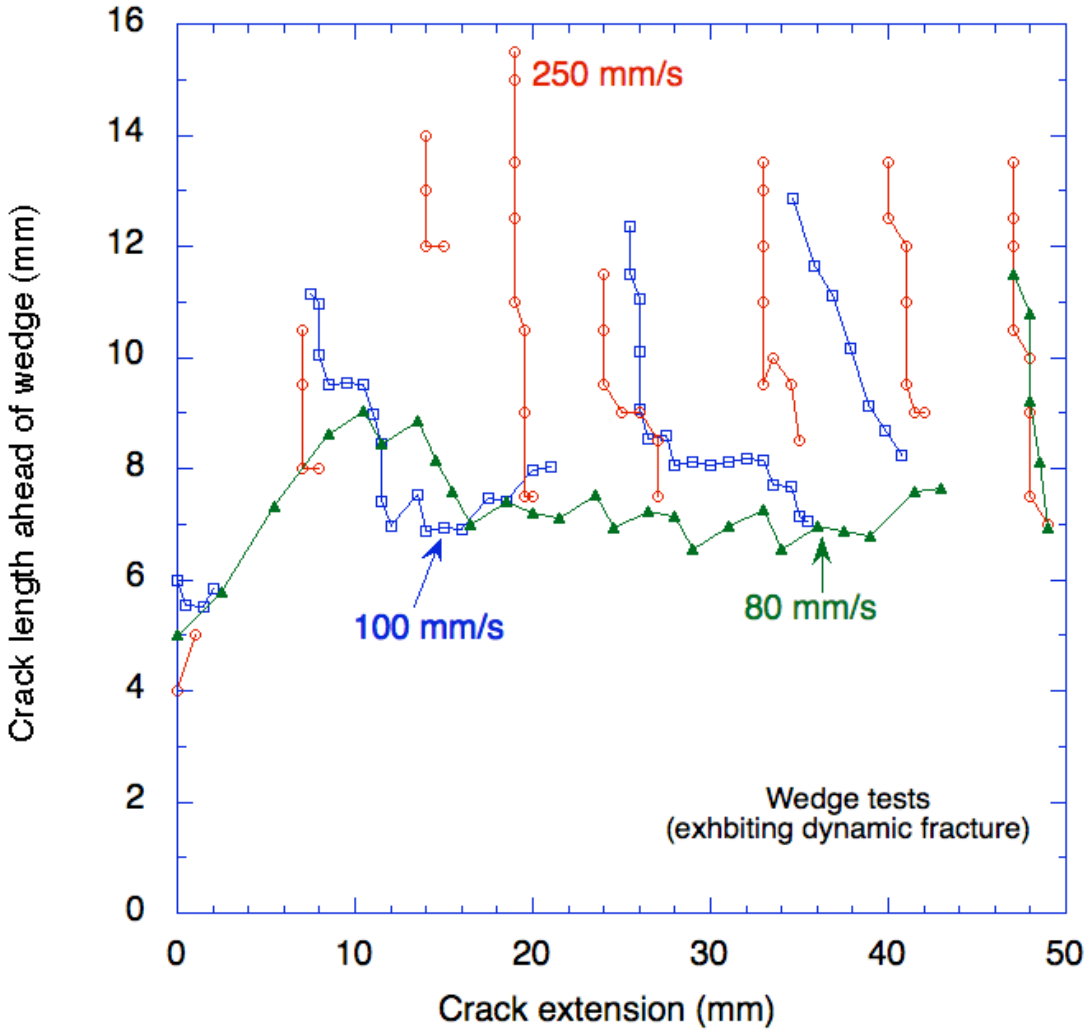
Crack length ahead of wedge (mm)
Crack extension (mm)
0
2
4
6
8
10
12
14
16
0
10
20
30
40
50
250 mm/s
100 mm/s
80 mm/s
Wedge tests
(exhbiting dynamic fracture)

Figure 10b

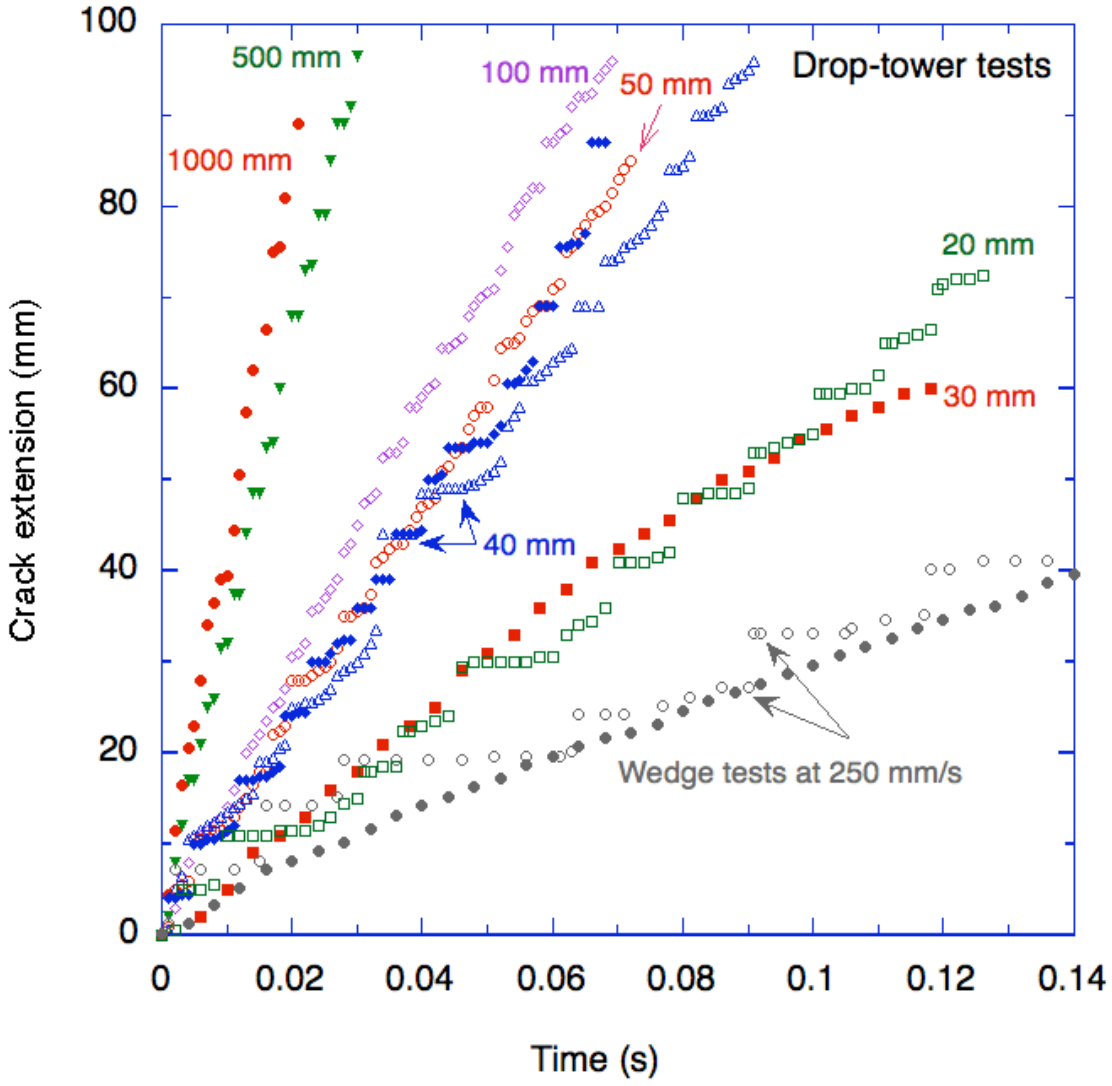
Crack extension (mm)
Time (s)
Drop-tower tests
500 mm
1000 mm
100 mm
50 mm
20 mm
30 mm
40 mm
Wedge tests at 250 mm/s
0
20
40
60
80
100
0
0.02
0.04
0.06
0.08
0.1
0.12
0.14

Figure 11

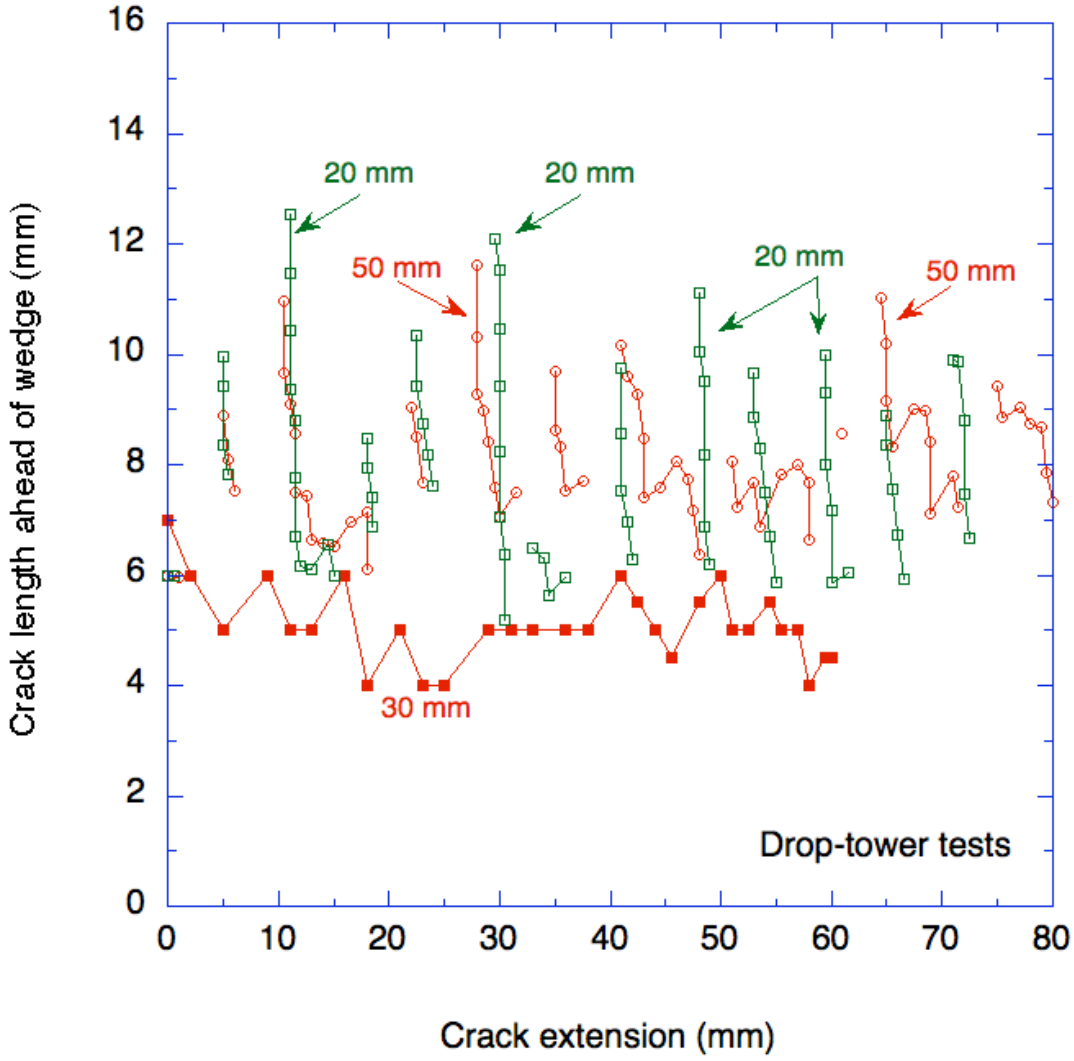
Crack length ahead of wedge (mm)
Crack extension (mm)
20 mm
20 mm
20 mm
50 mm
50 mm
30 mm
Drop-tower tests
0
2
4
6
8
10
12
14
16
0
10
20
30
40
50
60
70
80

Figure 12

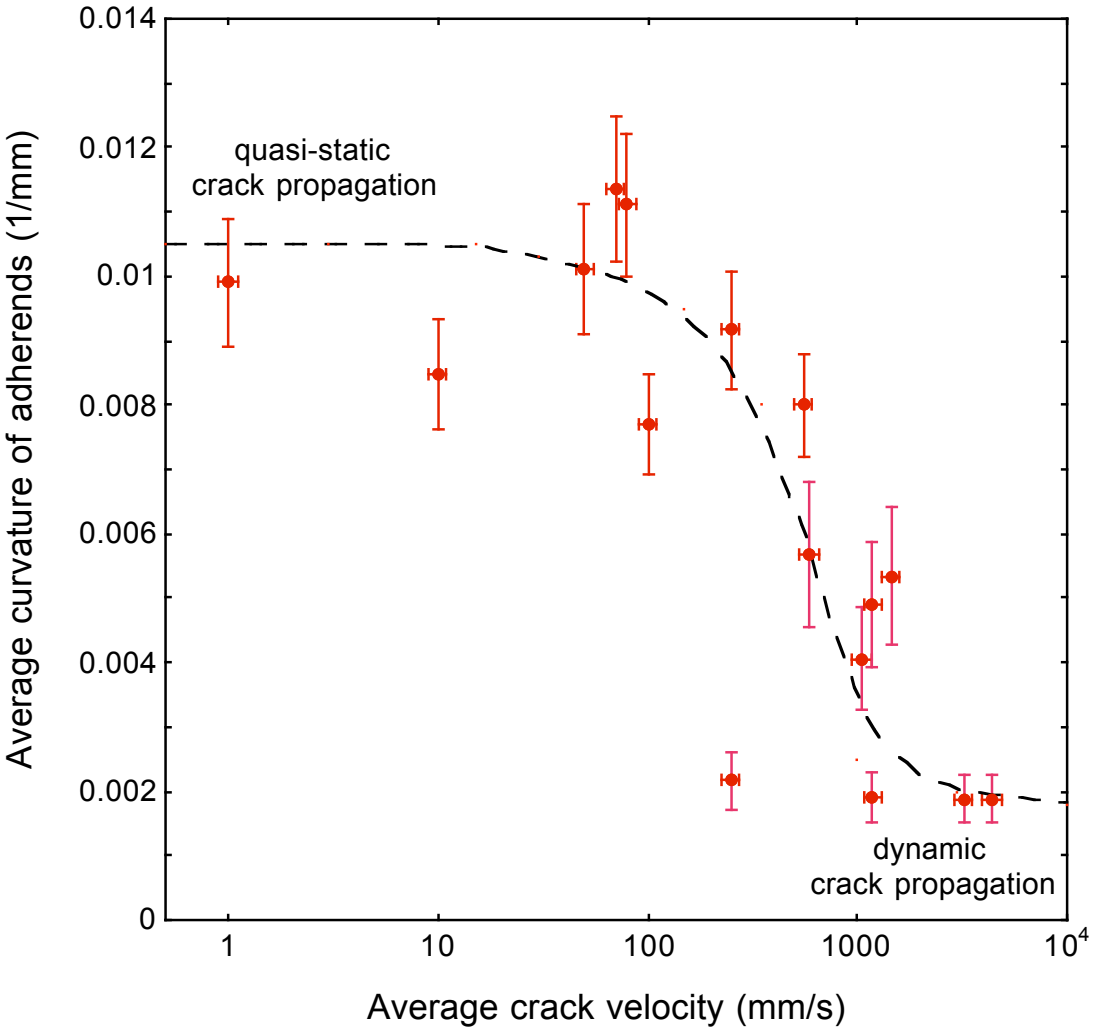
0.014
0.012
0.01
0.008
0.006
0.004
0.002
0
Average curvature of adherends (1/mm)
quasi-static
crack propagation
dynamic
crack propagation
1
10
100
1000
10^4
Average crack velocity (mm/s)

Figure 13a

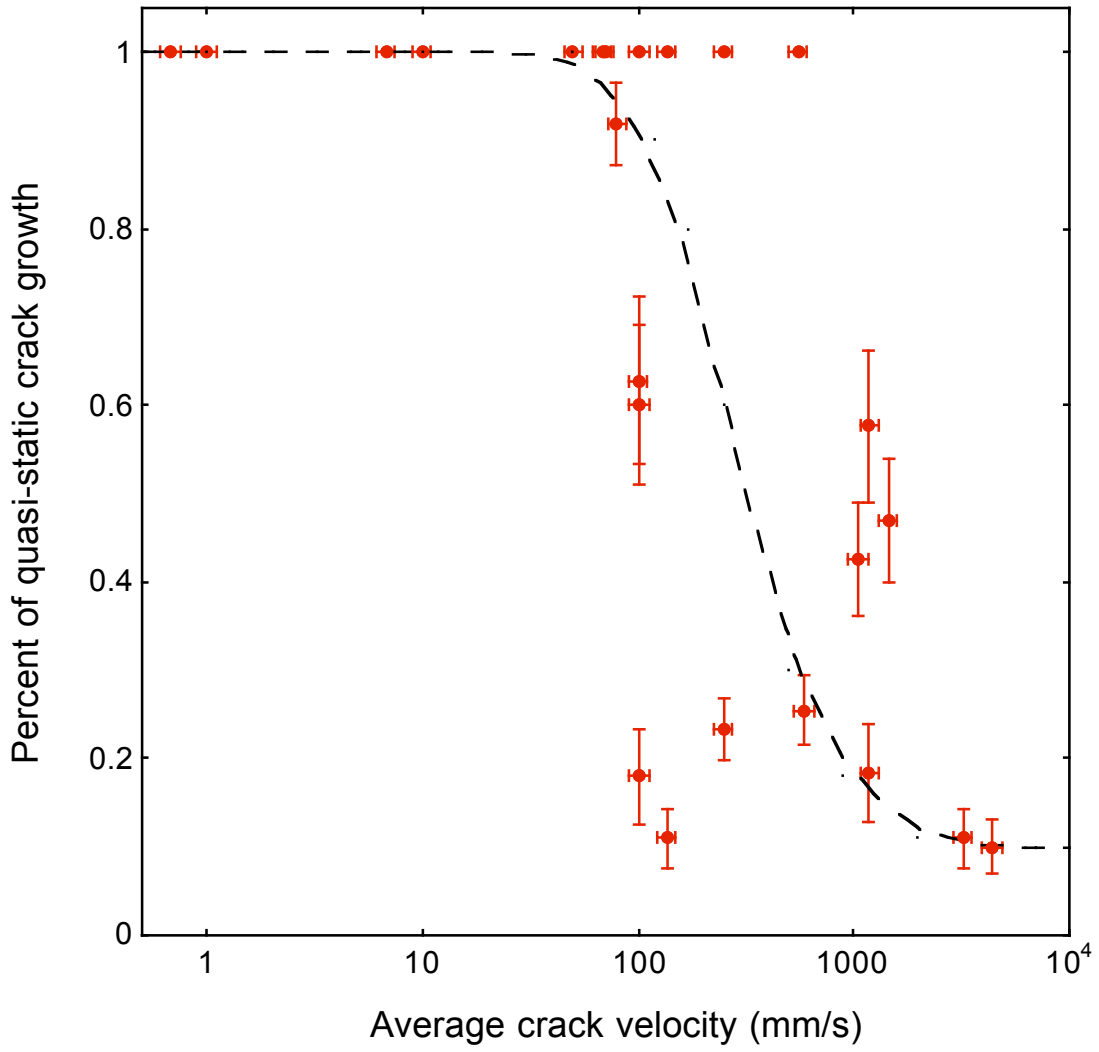
Percent of quasi-static crack growth
1
0.8
0.6
0.4
0.2
0
1
10
100
1000
10^4
Average crack velocity (mm/s)

Figure 13b